

On the Use of Finite Surfaces in the Numerical Prediction of Rough Surface Scattering

Roger T. Marchand, *Member, IEEE*, and Gary S. Brown, *Fellow, IEEE*

Abstract—Method of moments (MOM)-based Monte Carlo calculations are widely used in determining the average radar cross section of randomly rough surfaces. It is desirable in these numerical calculations to truncate the scattering surface into as short a length as possible to minimize the solution time. However, truncating the surface tends to change the solution for the surface fields near the truncation points and may alter the scattered far fields. In this paper, these end effect errors are examined for one-dimensional (i.e., grooved or corduroy) surfaces which are Gaussian distributed in height and have either a Gaussian or a Pierson–Moskowitz spectra. In the case of the Pierson–Moskowitz type surface, it is shown that a relatively short surface of 80–120 wavelengths can be used to obtain the average backscattered radar cross section for backscattering angles as large as 60° from normal. For a comparatively smooth Gaussian surface, on the other hand, it is shown that the truncation effects can be very significant at moderate backscattering angles. Also, great care should be taken when examining the scattering from Gaussian surfaces which are dominated by specular scattering. It is shown that in this situation, a very large number of calculations may be needed to obtain a good numerical average.

Index Terms—End effects, method of moments, rough surface scattering.

I. INTRODUCTION

MONTE CARLO calculations for the average radar cross section of randomly rough surfaces have been used by a number of researchers for more than a decade [1]–[8], [10]–[12]. Typically such calculations are performed using a surface integral equation formulation of the scattering problem in combination with a random surface generator and the method of moments (MOM, sometimes referred to as the boundary element method or the method of weighted residuals). In the method of moments approach, the surface fields (or surface currents) are approximated by a set of functions, which are called basis functions. For rough surface scattering problems, the basis functions are often chosen as set of current pulses. In effect, the integral equation is approximated by a matrix equation which can be solved using standard matrix techniques. A significant difficulty with this approach is that: 1) the MOM matrix is a full matrix (i.e., it is not sparse) and 2) in order to obtain accurate results the basis functions must be quite small, typically on the order of one-tenth the size of the incident wavelength or less [1], [8], [10], [12]. Regardless of whether the resulting matrix equation is solved using traditional matrix equation solvers, such as

lower upper (LU) triangular matrix decomposition, or iterative techniques, such as the conjugate gradient technique, the method of ordered multiple interactions (MOMI), or the fast multipole method, the time required to solve the matrix equation increases rapidly as the length of the scattering surface increases [1], [3]. The time required using LU decomposition, for example, scales as the L^3 (where L is the length of the scattering surface), while iterative techniques generally scale between L^2 and $L \log(L)$ for each iteration, depending on the technique. It is therefore desirable to truncate the scattering surface used in the numerical calculation into as short a surface as possible to minimize the solution time. However, truncating the surface generally causes numerical errors in the solution for the surface fields near the truncation points and in some circumstances may eliminate important contributions to the scattered field. In order to reduce these end effect errors, a tapered incident field is frequently used. Examples of such end effect errors and tapering limitations are presented in Section II.

Also, a serious limitation to any Monte Carlo simulation is the possibility that some important events may be sufficiently unlikely to occur that they are difficult to include in the simulation. In Section III, it is shown that such a situation is encountered when calculating the average radar cross section of finite length surfaces with Gaussian spectra, large root mean squared (rms) height and small rms slope.

II. END EFFECTS

Let us first consider the simple case of a perfectly flat finite length one-dimensional surface. Fig. 1 plots the magnitude of the electric surface current obtained from a method of moments (MOM) solution of the electric field integral equation, (1), under various illuminations. A detailed description of the MOM implementation for this equation can be found in [7] and [10].

$$E_i(\vec{r}) = \int G(\vec{r}, \vec{r}_o) \frac{\partial E(\vec{r}_o)}{\partial n_o} dS_o \quad (1)$$

where $E_i(\vec{r})$ is the incident electric field, $\partial E(\vec{r}_o)/\partial n_o$ is the unknown surface current (n_o being the surface normal vector at the point \vec{r}_o), $G(\vec{r}, \vec{r}_o) = -0.25jH_0^{(2)}(k|\vec{r} - \vec{r}_o|)$ is the one-dimensional Greens function, $k = 2\pi/\lambda$ is the magnitude of the incident wave vector $\vec{k} = k\hat{k} = k[\hat{x} \sin \theta_i + \hat{z} \cos \theta_i]$, λ is the electromagnetic wavelength, θ_i is the incident angle and $H_0^{(2)}()$ is the zeroth-order Hankel function of the second kind.

Manuscript received March 27, 1998.

The authors are with the Department of Meteorology, The Pennsylvania State University, University Park, PA 16802 USA.

Publisher Item Identifier S 0018-926X(99)04788-2.

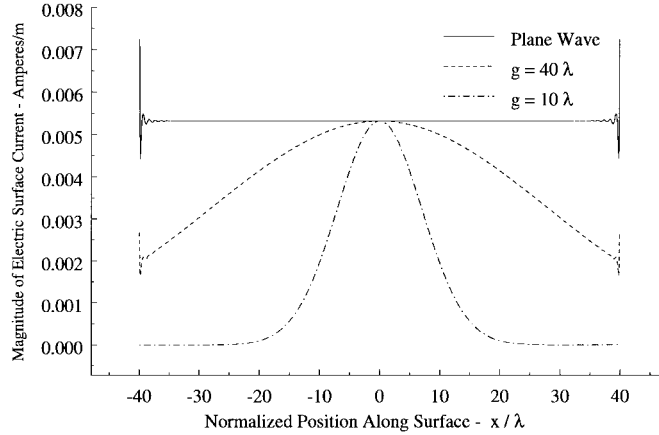


Fig. 1. Magnitude of the electric surface current on a flat surface 80λ long under plane wave and tapered illumination. (The calculations use $\Delta x = 0.1\lambda$, $\theta_i = 0^\circ$, and TE polarization.)

The figure shows that the solution obtained using plane wave illumination (solid line) contains large spikes in the current at the ends of the surface. Because the far-field transformation (essentially a Fourier transform) of a delta function is a constant and the Fourier transform of a constant current over a finite length is the well known sinc function, the plane wave illumination of the finite-length surface results in a radar cross section which is a sinc function plus a broadly dispersed (in angle) component due to the end currents. This is not to infer that this sinc-like solution is not the correct solution for the scattering from a finite-length surface. The essential point is that we are interested in the scattered field for a surface which is not truncated. The truncation is a limitation of the numerical solution technique and not a part of the problem of interest and so we desire to minimize the effects of the finite surface truncation.

For a flat surface, suppressing the end effects is easily achieved by tapering the incident field. One such tapering introduced by Thorsos [10] has been widely used [3], [6], [8]

$$E_i(\vec{r}) = \exp[-j(1+w(\vec{r}))\hat{k} \cdot \vec{r} - (x - z \tan \theta_i)^2/g^2] \quad (2)$$

where $w(x, z) = (2(x - z \tan \theta_i)^2/(g^2 - 1))/(kg \cos \theta_i)^2$ and the parameter “ g ,” called the half-spot size, determines the length on the surface over which the magnitude of the incident field drops by a factor of $1/e$ from its maximum value. It should be noted, that (2) only approximately satisfies Maxwell’s equations, and there are conditions which limit the minimum g as a function of the incident angle (see the Appendix).

Fig. 1 shows that the tapered field reduces the current at the ends of the scattering surface. In this example, a tapering parameter of $g = 40\lambda$, yields smaller current spikes than those observed for the plane wave, while a spot size of 10λ produces no noticeable spikes (at least on a linear scale). For $g = 10\lambda$ the surface currents and the scattered fields will not change noticeably if the surface length is increased, and so in this sense we can say that the scattered field solution is free of end effects. (Of course, the scattered far field for the case of the tapered incident field is not a delta function, as one would obtain for an infinitely long surface under plane wave

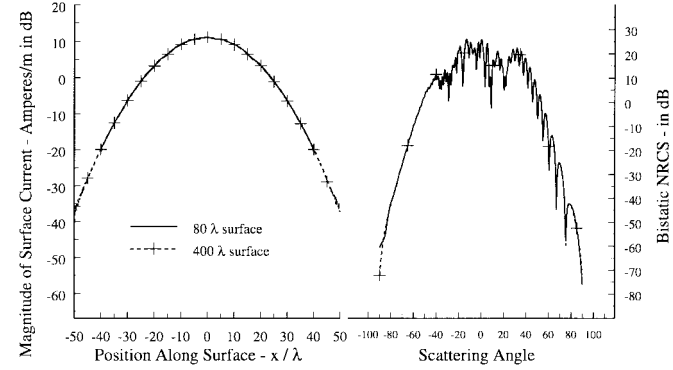


Fig. 2. Example of surface truncation effects for $\theta_i = 0^\circ$, using one realization of a PEC surface with a Gaussian spectrum, rms height (σ_h) = 0.707λ , and correlation length (L) = 4.5λ . (The calculations use $\Delta x = 0.1\lambda$, $\theta_i = 0^\circ$, TM polarization, and $g = 15\lambda$.)

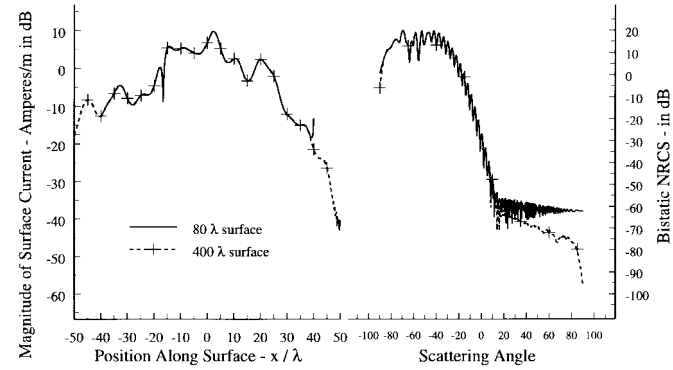


Fig. 3. Same as Fig. 2 but with $\theta_i = 70^\circ$.

illumination, but has a Gaussian-like shape. There is an inverse relationship between the length of the illuminated surface and the width of this Gaussian-like pattern.)

For rough surfaces, on the other hand, the incident field may be scattered by the surface roughness along the surface such that it reaches the ends of the truncated surface. Consequently, tapering the incident field does not guarantee that the fields at the ends of the truncated surface are small. This problem becomes increasingly difficult as the incident angle approaches grazing incidence. For example, Figs. 2 and 3 plot the magnitude of the electric surface current and the normalized radar cross section (NRCS), normalized by incident power as in [3], for one realization of a rough PEC which is truncated at 80 and at 400 wavelengths. The particular surface used these calculations is depicted in Fig. 4 (left side). Examining the surface current reveals that when the incident angle is 0° (Fig. 2) there is very little current outside the primary illumination region (roughly $|x| < 2g$) and correspondingly this is very little difference in the radar cross sections for the two surface lengths. However, when the incident angle is 70° (Fig. 3), the scattered field propagates along the surface much more than 40 wavelengths and consequently there are very significant changes in the radar cross section for the two surface lengths, especially where the radar cross section is small.

This end effect is usually easy to identify when examining the backscattered radar cross section. Fig. 4 (right side),

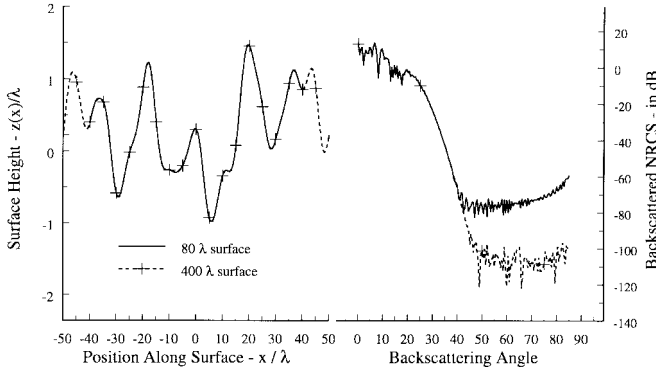


Fig. 4. (left side) Depiction of the Gaussian rough surface used in the calculations displayed in Figs. 2–4. (right side) Backscattered normalized radar cross section (NRCS).

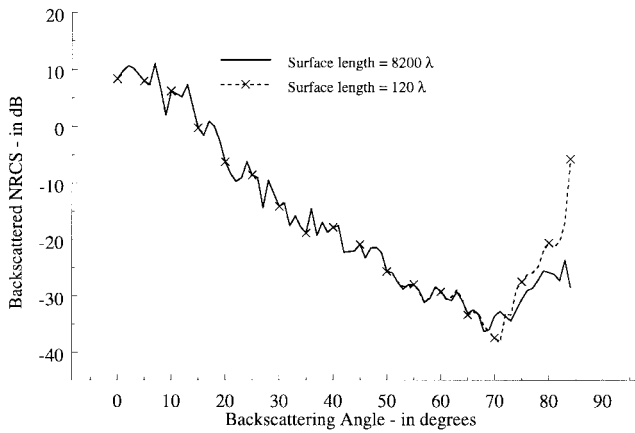


Fig. 5. Surface truncation effects on the average backscattered NRCS from ten realizations of surfaces with Pierson–Moskowitz spectra. [The calculations use a wind speed ($U_{19.5}$) = 15 m/s, $\lambda = 0.10$ m, surface spectral cutoff (k_c) = $2k_0$, $\Delta x = 0.15\lambda$, TE polarization, and $g = 15\lambda$.]

for example, plots the backscattered normalized radar cross section (NRCS) for the same surface used in Figs. 2 and 3. The backscattered cross sections for both surface lengths are in good agreement up to about 40° . In this angular region, the backscattered NRCS is accurate because the contribution from the illuminated surface is much greater than the contribution from the region near the surface edges.

The above example was chosen for its pronounced end effects. The end effects are not always this significant. Fig. 5, for example, compares the average backscattered radar cross section computed from ten surfaces with Pierson–Moskowitz spectra, where the scattering surface has been truncated at two different lengths of 8200 and 120 wavelengths. This figure shows that there is very good agreement between the two solutions down to incident angles of about 60° . (The breakdown in the solution for angles greater than about 70° , is directly related to an insufficiently large value for incident field tapering parameter, g . If g is increased this problem is eliminated, see Fig. 6.) In fact, we have observed that for these Pierson–Moskowitz type surfaces, surface lengths as short as 80 wavelengths with g set to 15 wavelengths produces good results for the backscattered radar cross section to 60° .

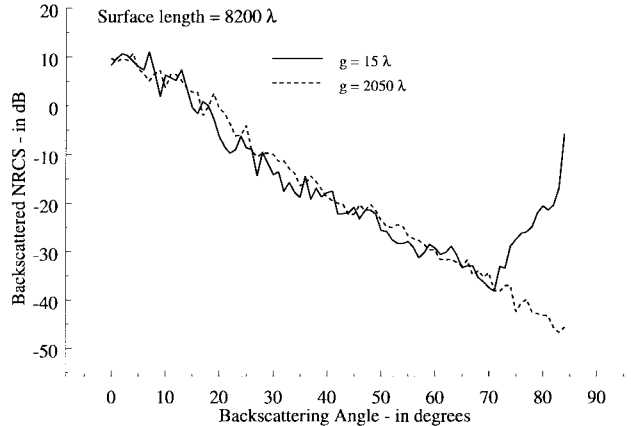


Fig. 6. Same as Fig. 5 but with $g = 15\lambda$ and $g = 2050\lambda$.

A large part of the reason why the far field in Fig. 5 is seemingly unaffected by the surface truncation is simply that the Pierson–Moskowitz surface contains considerable Bragg scattering elements which give rise to a much larger backscattered field than does the relatively smooth Gaussian surface. So even though one might expect the rougher Pierson–Moskowitz surface to have larger errors in the surface currents, these errors are not significant in the far field.

In general, we have observed that the edge effects depend slightly on the polarization, the nature of the surface roughness, the integral equation used, the matrix solver (e.g., LU decomposition versus MOMI) and the sampling density. In regards to iterative matrix solvers, presumably truncating the iterative series produces different end effects because each technique has different “orderings” of the scattering process.

The important conclusion to be drawn here is that although tapering the incident field can substantially reduce end effects, they are not completely eliminated and extra care should be taken whenever the calculated radar cross section is small. In our research, a minimum value for g of ten wavelengths or $g > 5/k(\pi/2 - |\theta_i|) \cos \theta_i$ (whichever is larger) and a total surface length of four to six times g was observed to be an effective threshold for backscattering angles up to 80° from normalized radar cross sections greater than about -60 dB.

III. FINITE-LENGTH MONTE CARLO RUNS

The scattering from Gaussian rough surfaces that do not contain any significant variations in their height on spatial scales ten times the length of the incident wavelength or shorter are dominated by specular (i.e., ray-like) scattering [7]. However, these surfaces may contain important specular facets (i.e., slopes) which occur very infrequently. For example, Fig. 7 compares the theoretical probability density function (pdf) with two estimated slope pdf's (essentially histograms of the slope) for randomly generated surfaces which are Gaussian distributed in height and have a Gaussian spectra with a rms height of 2.24λ and rms slope of 24.1° . The slope given along the horizontal axis of this figure is the rate of change in the height of the rough surface with respect to the mean scattering surface (plane). (This value can be converted into the angle

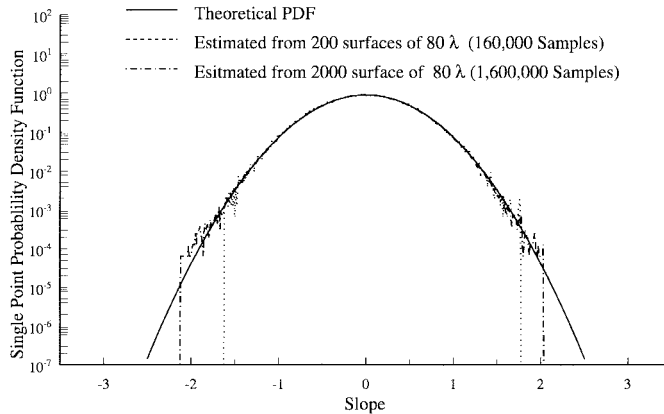


Fig. 7. Histograms of the surface slopes for finite length surfaces with Gaussian spectra [$\sigma_h = 2.24\lambda$ and rms slope (σ_s) = 24.1°]. Slope estimates obtained via difference formula with $\Delta x = 0.1\lambda$.

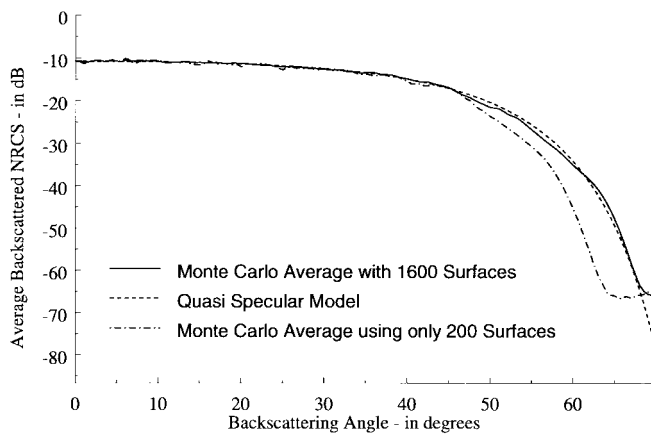


Fig. 8. The average NRCS for the same surfaces examined in Fig. 7. [Calculations use a dielectric constant (ϵ_r) = 2.0, TM polarization, a surface length of 80λ and $g = 15\lambda$].

formed between a line with this slope and the mean scattering plane by taking its tangent, i.e., $\theta = \tan \zeta_x$.) Fig. 7 shows that when 200 surfaces which were 80 times longer than the incident wavelength were examined, no slope greater than about 1.7 was found. As a result, none of the 200 surfaces contained a slope which could specularly backscatter a ray incident at 60° . When the number of surfaces examined was increased to 2000, a few slopes of up to 2.1 were found. These slopes can back reflect rays up to about 65° . Note that this is not an error in the surface generation program. For this example, the likelihood that a point on the surface will have a slope of two or greater is $3.385 \times 10^{-4}\%$. When the large slopes are not included in the Monte Carlo sample population, the average backscattered radar cross section is significantly underestimated at large backscattering angles, as shown in Fig. 8.

IV. SUMMARY

The time required to solve the MOM matrix equation increases as the length of the scattering surface increases. It is therefore desirable to truncate the scattering surface used in the numerical calculations into as short a surface as

possible to minimize the solution time. However, truncating the surface generally causes numerical errors in the solution for the surface fields near the truncation points and in some circumstances may alter the scattered far field. Although tapering the incident field can substantially reduce the end effects, they are not completely eliminated and extra care should be taken whenever the calculated radar cross section is small. Conditions which the authors have found effective in suppressing end effects for surfaces with Pierson–Moskowitz and Gaussian spectra are described in Section II.

Finally, a serious limitation to any Monte Carlo simulation is the possibility that some important events may be sufficiently unlikely to occur that they will not be properly included in the simulation. Section III demonstrates that such a situation is encountered when calculating the averaged radar cross section of finite length surfaces with Gaussian spectra, large rms height, and small rms slope.

APPENDIX

One possible incident field tapering, derived by Thorsos [10], was given in Section II as (2). Thorsos' derivation of (2) starts with an angular spectrum of plane waves representation for the incident field. That is, the incident field is given by a sum of plane waves traveling in different directions with a Gaussian weight

$$E_i(\vec{r}) = \frac{2}{\sqrt{\pi}(kg \cos \theta_i)} \int_{-\pi/2}^{\pi/2} \exp \left[\frac{-(\theta' - \theta_i)^2}{4/(kg \cos \theta_i)^2} \right] \cdot \exp[-j\vec{k}_i \cdot \vec{r}] d\theta'. \quad (\text{A.1})$$

Equation (2) is then obtained from (A1) by: 1) performing a change of variables, $\delta = \theta' - \theta$; 2) extending the limits of integration to infinity; and 3) expanding the term $\vec{k}_i \cdot \vec{r} = k[-\cos(\theta' - \delta)z + \sin(\theta' - \delta)x]$ in δ , and retaining terms up to order δ^2 . Thorsos states that the resulting equation is accurate to order $1/(kg \cos \theta_i)^2$. However, in extending the limits beyond $\pi/2$, Thorsos has allowed for contributions to the incident field representing plane waves with incident angles greater than 90° . Therefore, an additional constraint must be placed on g to prevent any “significant” incident field contribution from these unrealistic incident angles. A reasonable form for this condition is given as follows:

$$g > \frac{A\sqrt{2}}{k(\pi/2 - |\theta_i|) \cos \theta_i} \quad (\text{A.2})$$

where “ A ” is a constant which specifies how much the incident field spectrum has drooped (at grazing incidence) from its peak value at θ_i . In our research, a value for “ A ” of three to four was observed to be an effective threshold for backscattering angles down to roughly 80° , although this may depend on the surface spectrum. At incidence angles away from normal, this additional constraint dominates the condition given by Thorsos. When Thorsos' approximate incident field can not be used, one can numerically evaluate an angular spectrum of plane waves equation, such as (A.1), to obtain the incident field [9].

REFERENCES

- [1] P. Cao and S. Macaskill, "Iterative techniques for rough surface scattering problems," *Wave Motion*, vol. 21, p. 209.
- [2] K. Fung and M. F. Chen, "Numerical simulations of scattering from simple and composite random surfaces," *J. Opt. Soc. Amer. A*, vol. 2, no. 12, p. 2274.
- [3] D. A. Kapp and G. S. Brown, "A new numerical method for rough-surface scattering calculations," *IEEE Trans. Antennas Propagat.*, vol. 45, p. 711.
- [4] Y. Kim, E. Rodriguez, and S. L. Durden, "A numerical assessment of rough surface scattering theories: Horizontal polarization," *Radio Sci.*, vol. 27, no. 4, p. 497.
- [5] ———, "A numerical assessment of rough surface scattering theories: Vertical polarization," *Radio Sci.*, vol. 27 no. 4, p. 515.
- [6] A. A. Maradudin, E. R. Mendez, and T. Michel, "Backscattering effects in the elastic scattering of p-polarized light from a large-amplitude random metallic grating," *Opt. Lett.*, vol. 14, no. 3, p. 151, 1989.
- [7] R. T. Marchand, "A numerical study on the validity of the quasiespecular and two-scale models for rough surface parameter estimation: One dimensional surfaces," Ph.D. dissertation, Virginia Tech, 1997.
- [8] M. Nieto-Vesperians, *Scattering and Diffraction in Physical Optics*. New York: Wiley, 1991.
- [9] C. L. Rino and H. D. Ngo, "Forward propagation in a half-space with an irregular boundary," *IEEE Trans. Antennas Propagat.*, vol. 45, p. 1340, 1997.
- [10] E. I. Thorsos, "The validity of the Kirchhoff approximation for rough surface scattering using a Gaussian roughness spectrum," *J. Acoust. Soc. Amer.*, vol. 83, p. 78, 1988.
- [11] ———, "Acoustic scattering from a 'Pierson-Moskowitz' sea spectrum," *J. Acoust. Soc. Amer.*, vol. 88, no. 1, p. 335, 1990.
- [12] J. V. Toporkov, R. T. Marchand, and G. S. Brown, "On the discretization of the integral equation describing scattering by rough conducting surfaces," *IEEE Trans. Antennas Propagat.*, vol. 46, p. 150, 1998.



Roger T. Marchand (S'92–M'93) received the B.S., M.S., and Ph.D. degrees in electrical engineering from Virginia Tech, Blacksburg, in 1990, 1993, and 1997, respectively.

Since March 1997, he has been a Research Associate at the Pennsylvania State University Department of Meteorology. He is currently involved in a number of research projects concerned with remote sensing of the Earth's atmosphere and surface. In particular, his research focus has been on improving the understanding of cloud radiative properties using

millimeter wave radar and various passive remote sensing instrumentation, including satellite-based sensors. He is also a member of the Multiangle Imaging Spectro-Radiometer (MISR) Science Team. MISR is one of several instruments, which will be launched by NASA in 1999 as part of its EOS project.

Gary S. Brown (S'61–M'67–SM'81–F'86) received the B.S. E. E. degree in 1963, the M.S.E.E. degree in 1964, and the Ph.D. degree in 1967, all from the University of Illinois, Urbana-Champaign.

Dr. Brown was an Associate Editor of the IEEE TRANSACTIONS ON ANTENNAS AND PROPAGATION and the IEEE JOURNAL OF OCEANIC ENGINEERING from 1979 to 1988. He was President of the IEEE Antennas and Propagation Society in 1988 and has been a member of the society's Fellows Committee and Meetings Committee from 1994 to the present and the society's Press Relations Committee from 1993 to the present.